Free Radical Biology and Medicine 210 (2024) 333–343

Contents lists available at ScienceDirect

Free Radical Biology and Medicine

journal homepage: www.elsevier.com/locate/freeradbiomed

Selenite ameliorates the ATP hydrolysis of mitochondrial F_1F_O-ATPase by changing the redox state of thiol groups and impairs the ADP phosphorylation

Cristina Algieri [a,1], Francesca Oppedisano [b,1], Fabiana Trombetti [a], Micaela Fabbri [a], Ernesto Palma [b], Salvatore Nesci [a,*]

[a] Department of Veterinary Medical Sciences, Alma Mater Studiorum-University of Bologna, 40064, Ozzano Emilia, Italy
[b] Department of Health Sciences, Institute of Research for Food Safety and Health (IRC-FSH), University "Magna Græcia" of Catanzaro, 88100, Catanzaro, Italy

ARTICLE INFO

Keywords:
Mitochondria
F_1F_O-ATPase
Selenite
Thiol groups
Oxidative phosphorylation

ABSTRACT

Selenite as an inorganic form of selenium can affect the redox state of mitochondria by modifying the thiol groups of cysteines. The F_1F_O-ATPase has been identified as a mitochondrial target of this compound. Indeed, the bifunctional mechanism of ATP turnover of F_1F_O-ATPase was differently modified by selenite. The activity of ATP hydrolysis was stimulated, whereas the ADP phosphorylation was inhibited. We ascertain that a possible new protein adduct identified as seleno-dithiol (-S-Se-S-) mercaptoethanol-sensitive caused the activation of F-ATPase activity and the oxidation of free –SH groups in mitochondria. Conversely, the inhibition of ATP synthesis by selenite might be irreversible. The kinetic analysis of the activation mechanism was an uncompetitive mixed type with respect to the ATP substrate. Selenite bound more selectively to the F_1F_O-ATPase loaded with the substrate by preferentially forming a tertiary (enzyme-ATP-selenite) complex. Otherwise, the selenite was a competitive mixed-type activator with respect to the Mg^{2+} cofactor. Thus, selenite more specifically bound to the free enzyme forming the complex enzyme-selenite. However, even if the selenite impaired the catalysis of F_1F_O-ATPase, the mitochondrial permeability transition pore phenomenon was unaffected. Therefore, the reversible energy transduction mechanism of F_1F_O-ATPase can be oppositely regulated by selenite.

1. Introduction

The rotational ATPase family member F-type ATP synthase (also known as F_1F_O-ATPase) is found in eukaryotic mitochondria, serving as both an ion pump and an ATP synthesis complex. The catalytic F_1 hydrophilic domain and the F_O transmembrane hydrophobic domain are the two main structural components of F_1F_O-ATPase [1–5]. Both a functional and a structural function are assigned to the F_O domain. It participates in the generation of ATP during oxidative phosphorylation (OXPHOS), and the supramolecular organization in dimers arrayed in a long row contributes to the development of mitochondrial *cristae* [6]. ADP and Pi are the substrates used to synthesize ATP in the mitochondria. Proton motive force (Δp), produced by the mitochondrial respiratory complexes, provides the energy needed for this reaction [7].

Furthermore, the creation of the mitochondrial permeability transition pore (mPTP), which is located in the inner mitochondrial membrane (IMM), is directly influenced by the F_O transmembrane domain [8,9]. Recently it has been demonstrated that a natural compound such as the bergamot polyphenolic fraction positively influences mitochondrial bioenergetic parameters, improving cellular oxidative metabolism [10]; as well as protecting porcine aortic endothelial cells from metabolic alterations caused by doxorubicin, an apoptosis-inducing anticancer agent [11]. Therefore, testing the effect of another naturally occurring compound, selenium seemed interesting. Although research in recent years has shown that selenium is an essential component for human health, it is a micronutrient that is only found in small amounts in our bodies. With oxygen, sulfur, and tellurium, selenium is a member of the group of oxoacids, group 16 of the periodic table. It is an element with properties of transition semimetals. It can be found in the environment in several states, such as elemental (Se^0), selenides (Se^{2-}), selenate (SeO_4^{2-}), or selenites (SeO_3^{2-}). It is an element characterized by the ease of transition to adjacent oxidation

* Corresponding author.
E-mail address: salvatore.nesci@unibo.it (S. Nesci).
[1] These authors contributed equally.

https://doi.org/10.1016/j.freeradbiomed.2023.11.041
Received 1 September 2023; Received in revised form 19 November 2023; Accepted 29 November 2023
Available online 4 December 2023

states, which are controlled by humidity, pH, free oxygen concentration, and redox potential [12]. Selenium is found in nature in numerous sources, including the soil, given the erosion of rocks containing the element; in plants, related to the quantity present in the soil; in water, from atmospheric deposits or soil drainage; in food and in the air, where it plays an important role in its biogeochemical cycle [12]. In living beings, it has an important structural and enzymatic role in some functions such as, for example, various antioxidant processes, the synthesis, metabolism and function of thyroid hormones. It is also necessary to properly function the immune system [13], showing antimutagenic, anti-inflammatory and antibacterial activity [14]. This element has multiple beneficial functions in our body. Therefore, its deficiency can lead to numerous physiological problems, including mood alterations, increased susceptibility to diseases such as pathologies involving oxidative stress and inflammation and an increased risk of tumour formation. Numerous selenium deficiency illnesses are frequently linked to a shortage of a different significant nutrient with antioxidant properties, such as vitamin E [14]. Selenium exhibits toxicity towards tumour cells, stimulating the apoptosis process in cell cultures and showing more significant toxicity towards malignant cells than benign ones. The mechanism of anticancer action is based on the induction of cell death through the production of superoxide radicals at the level of the mitochondria, which stimulates the mitochondrial pathway of apoptosis. It has been observed that this pathway induced by selenite is inhibited by overexpression of manganese superoxide dismutase, the concentration of which, in tumour cells, is relatively low compared to the healthy counterpart; therefore, it is possible to state that, in the prevention of tumours, selenium selectively induces apoptosis in tumour cells without causing significant damage to normal cells [14]. In other studies, it is reported that treatment with selenite causes damage to the mitochondria, leading to cell death [15].

Selenium is mainly incorporated into human physiology in the form of selenocysteine (Sec), and Sec-containing proteins are known as selenoproteins. Although all functional selenoproteins have redox active functions, Sec is also used for several biological roles. An example is glutathione peroxidase, belonging to a family of antioxidant enzymes able to perform the neutralization of hydrogen peroxide and organic hydroperoxides, in synergy with vitamin E, in the intracellular and extracellular compartments. The enzymatic activity is directly proportional to the intake of selenium; therefore, there is an important correlation between selenium deficiency and oxidative stress [12,14]. In particular, sodium selenite (Na_2SeO_3) is an inorganic form of the trace element selenium, commonly used for its potential neoplastic activity as it can induce apoptosis and inhibit the proliferation of cancer cells, as well as having various beneficial effects in the body. It has been demonstrated that selenite activates signalling pathways capable of stimulating mitochondrial biogenesis by increasing the synthesis of mitochondrial proteins [16].

Furthermore, selenite treatments significantly boost oxygen intake, enhancing the activities of the respiratory complexes and mitochondrial respiration. Additionally, selenite reduces free radical-induced apoptosis via influencing signalling pathways [16]. Exposure of cells to selenite prevents loss of mitochondrial membrane potential and metabolic activity, protecting cells from mitochondrial damage. Additionally, increased levels of ATP production in the mitochondrion have been observed in the presence of selenite [17]. It is known that F_1F_O-ATPase is inhibited by Mg-ADP, which, in the absence of phosphate, induces conformational changes on the catalytic portion of F_1, blocking Mg-ADP and preventing catalysis. A study on the coccoid bacterium *Paracoccus denitrificans* demonstrated that the phosphate-like selenite oxyanion can occupy phosphate binding sites on the F_1 domain or catalytic β-subunits or non-catalytic α-subunits, and induce conformational changes that allow the release of Mg-ADP, allowing ATP hydrolysis [18]. In the present study, the effects of selenite on F_1F_O-ATPase were investigated, as its modulating action on enzymatic activity and the effect on the mPTP are not yet known. The main aim was to determine the action of the compound on the enzyme by titration and shed light on the molecular mechanisms that can lead selenite to establish interactions with the thiol groups of F_1F_O-ATPase. For this purpose, both oxidizing and reducing reagents have been used.

2. Material and methods

2.1. Chemicals

Oligomycin (a mixture of oligomycins A, B and C), antimycin A, Fura-FF, glutamate, malate, and succinate were purchased from Vinci-Biochem (Vinci, Italy). Na_2ATP, ADP, rotenone, DL-dithiothreitol (DTT), 5,5′-Dithio-bis-(2-nitrobenzoic Acid) (DTNB), phenylarsine oxide (PAO), $HgCl_2$, 2-mercaptoethanol (ME), and sodium selenite were obtained from Sigma–Aldrich (Milan, Italy). Quartz double distilled water was used for all reagent solutions.

2.2. Preparation of the mitochondrial fractions

Swine hearts (*Sus scrofa domesticus*) were collected at a local abattoir and transported to the lab within 2 h in ice buckets at 0–4 °C. After removal of fat and blood clots as much as possible, approximately 30–40 g of heart tissue was rinsed in ice-cold washing Tris-HCl buffer (medium A) consisting of 0.25 M sucrose, 10 mM Tris(hydroxymethyl)-aminomethane (Tris), pH 7.4 and finely chopped into fine pieces with scissors. Each preparation was made from one heart. Once rinsed, tissues were gently dried on blotting paper and weighed. Then tissues were homogenized in medium B consisting of 0.25 M sucrose, 10 mM Tris, 1 mM EDTA (free acid), 0.5 mg/ml BSA fatty acid free, pH 7.4 with HCl at a ratio of 10 ml medium B per 1 g of fresh tissue. After a preliminary gentle break-up by Ultraturrax T25, the tissue was carefully homogenized by a motor-driven Teflon pestle homogenizer (Braun Melsungen Type 853,202) at 650 rpm with 3 up-and-down strokes. The mitochondrial fraction was then obtained by stepwise centrifugation (Sorvall RC2-B, rotor SS34). Briefly, the homogenate was centrifuged at 1,000×*g* for 5 min, thus yielding a supernatant and a pellet. The pellet was re-homogenized under the same conditions of the first homogenization and re-centrifuged at 1,000×*g* for 5 min. The gathered supernatants from these two centrifugations, filtered through four cotton gauze layers, were centrifuged at 10,500×*g* for 10 min to yield the raw mitochondrial pellet. The raw pellet was resuspended in medium A and further centrifuged at 10,500×*g* for 10 min to obtain the final mitochondrial pellet. The latter was resuspended by gentle stirring using a Teflon Potter Elvejehm homogenizer in a small volume of medium A, thus obtaining a protein concentration of 30 mg/ml [19]. All steps were carried out at 0–4 °C. The protein concentration was determined according to the colourimetric method of Bradford [20] by Bio-Rad Protein Assay kit II with BSA as standard. The mitochondrial preparations were then stored in liquid nitrogen until the evaluation of F_1F_O-ATPase activities.

2.3. Mitochondrial F-ATPase activity assays

Thawed mitochondrial preparations were immediately used for F-ATPase activity assays. The capability of ATP hydrolysis was assayed in a reaction medium (1 ml). The optimal conditions to obtain the maximal activity of the F_1F_O-ATPase, which depend on substrates concentration and pH values, are at 0.15 mg mitochondrial protein and 75 mM ethanolamine-HCl buffer pH 9.0, 6.0 mM Na_2ATP and 2.0 mM $MgCl_2$ for the Mg^{2+}-activated F_1F_O-ATPase assay, and 75 mM ethanolamine-HCl buffer pH 8.8, 3.0 mM Na_2ATP and 2.0 mM $CaCl_2$ for the Ca^{2+}-activated F_1F_O-ATPase assay [21,22]. These assay conditions were previously proven to elicit the maximal enzyme activities either stimulated by Mg^{2+} or by Ca^{2+} in swine heart mitochondria [23]. After 5 min pre-incubation at 37 °C, the reaction carried out at the same temperature, was started by the addition of the substrate Na_2ATP and stopped after 5

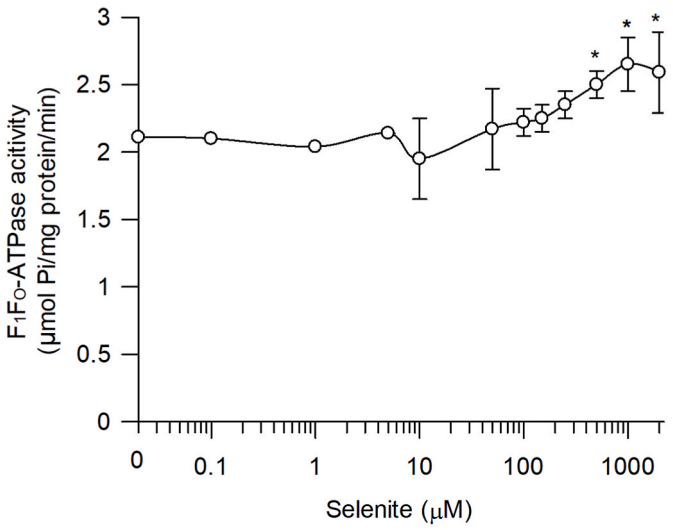

Fig. 1. Dose-response curve of selenite on the F_1F_O-ATPase activity. ATP hydrolysis in the presence of increasing selenite concentrations. Data represent the mean ± SD from three independent experiments carried out on distinct mitochondrial preparations. * indicate significantly different values within each treatment ($P \leq 0.05$).

min by the addition of 1 ml of ice-cold 15 % (w/w) trichloroacetic acid (TCA) aqueous solution. Once the reaction was stopped, vials were centrifuged for 15 min at 3500 rpm (Eppendorf Centrifuge 5202). In the supernatant, the concentration of inorganic phosphate (Pi) hydrolyzed by known amounts of mitochondrial protein, which is an indirect measure of F-ATPase activity, was spectrophotometrically evaluated [24]. According to the method employed, to detect the Pi release by the enzymatic reaction, the Pi released independently of the F_1F_O-ATPase activity should be quantified. To this aim, 1 µl from a stock solution of 3 mg/ml oligomycin in dimethylsulfoxide was directly added to the reaction mixture before starting the reaction. The total ATPase activity was calculated by detecting the Pi in control tubes run in parallel and containing 1 µl dimethylsulfoxide per ml reaction system. In each experimental set, control tubes were alternated to the condition to be tested. The employed dose of oligomycin, a specific inhibitor of F-ATPases which selectively blocks the F_O subunit ensured maximal enzyme activity inhibition and was currently used in F-ATPase assays [22].

To test the effect of selenite on the differently activated F_1F_O-ATPase activities, aqueous solutions of selenite at different standard concentrations were prepared immediately before each experimental set. Small aliquots (10 µl) of these solutions were added to the reaction system and incubated at 37 °C before starting the F_1F_O-ATPase reaction. Control tubes contained the same final volume, adjusted with 10 µl of the reaction buffer.

In all experiments, the F_1F_O-ATPase activity was routinely measured by subtracting, from the Pi hydrolyzed by total ATPase activity, the Pi

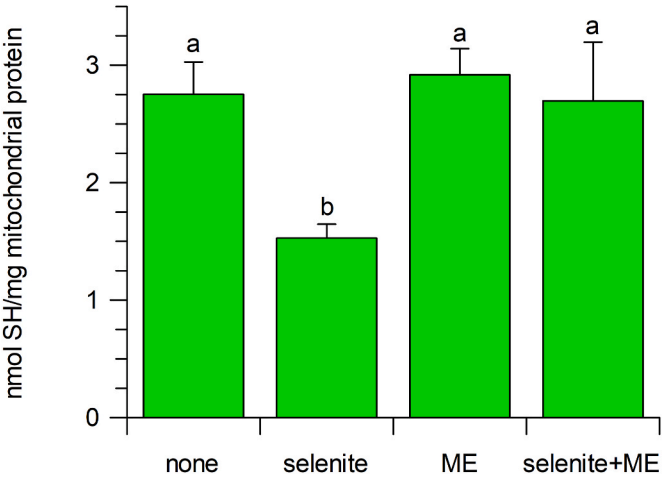

Fig. 3. Available mitochondrial protein single bond –SH groups in the absence or in the presence of 1 mM selenite and/or 400 mM mercaptoethanol (ME). Data are expressed as mean ± SD of four experiments carried out on mitochondria from different preparations. Different letters indicate significantly different values between treatments at $P \leq 0.05$.

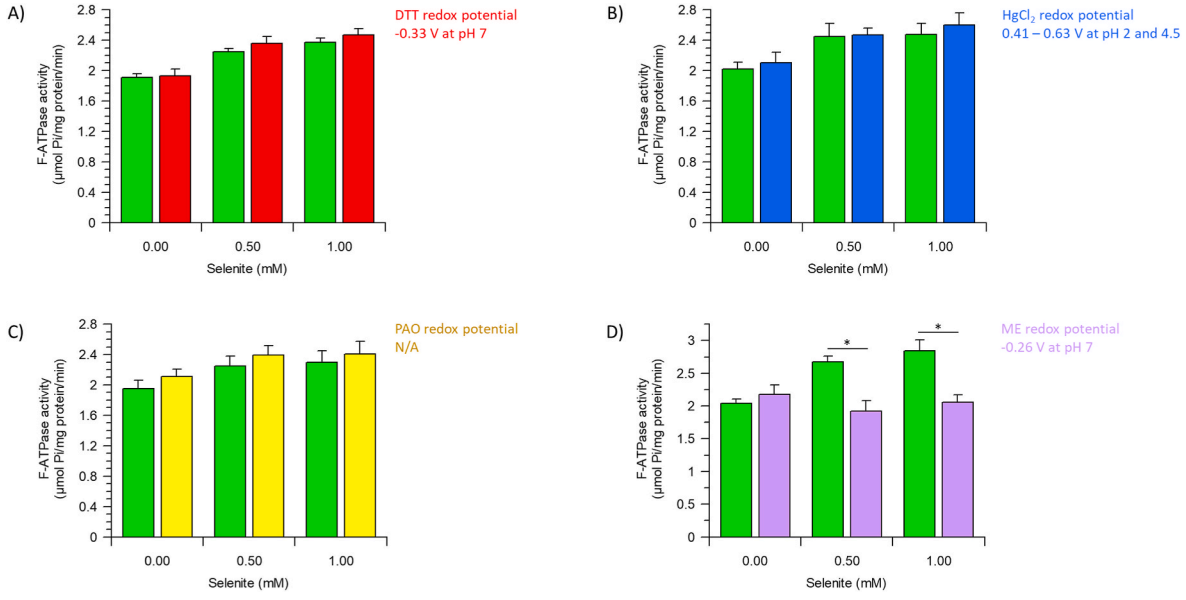

Fig. 2. F_1F_O-ATPase activity in selenite-treated mitochondria with and without thiol redox agent. The effect of increased selenite concentration was evaluated in the absence (green bars,) and in the presence) of (A) 50 µM DTT (red bars,), (B) 2.5 µM $HgCl_2$ (blue bars,), (C) 50 µM phenylarsine oxide, (yellow bars,), (D) 400 mM mercaptoethanol (lavender bars,). Data represent the mean ± SD from three independent experiments carried out on three different mitochondrial preparations. * indicate significantly different values within each treatment ($P \leq 0.05$).

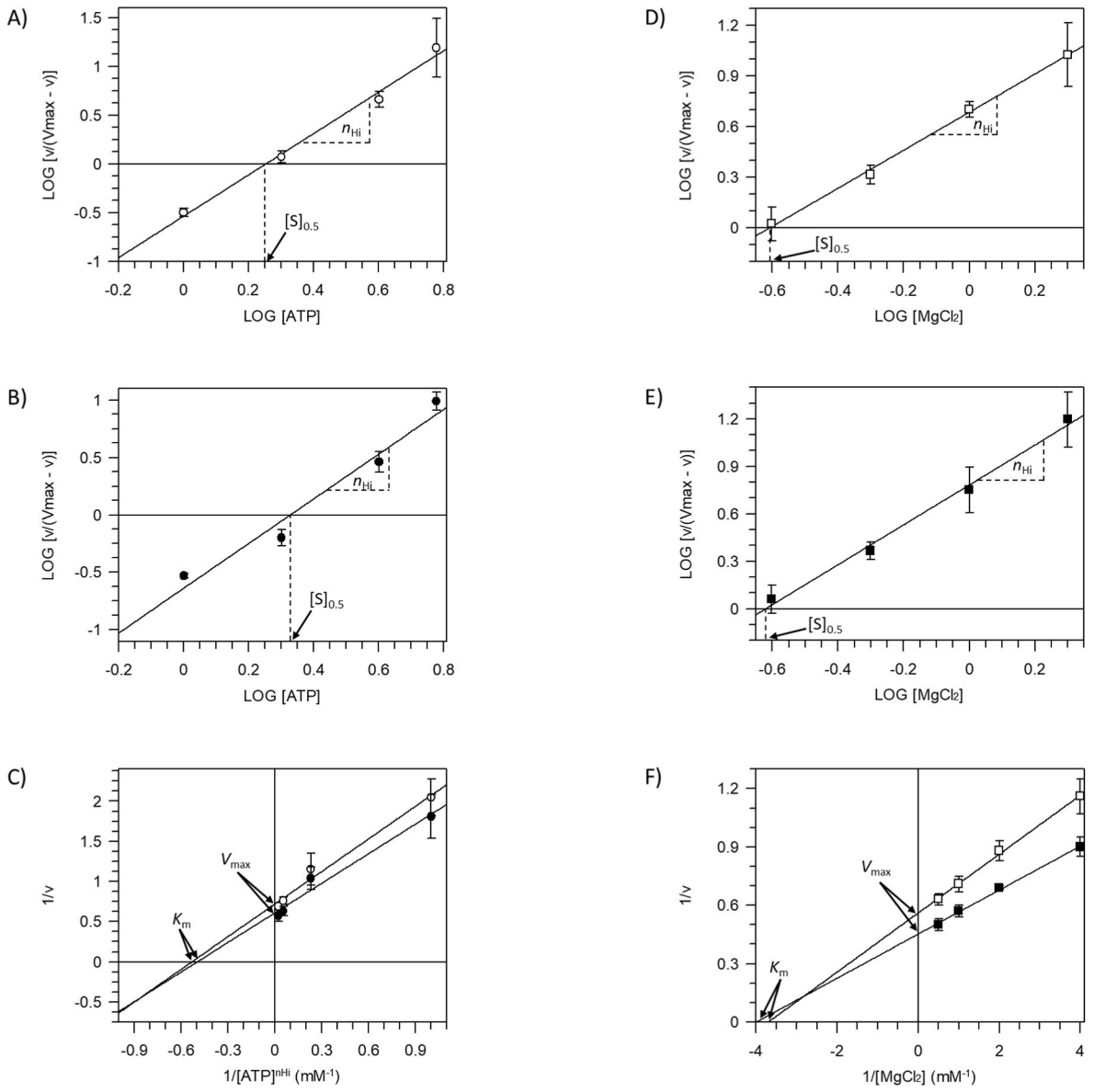

Fig. 4. Plots to obtain the kinetic parameters of the mitochondrial F_1F_O-ATPase. Hill plots to obtain the *n*Hi and [S]0.5 of the F_1F_O-ATPases related to ATP in the absence (A) or with 1 mM selenite (B) or Mg2+ in the absence (D) or with 1 mM selenite (E). Lineweaver-Burk plots of the F_1F_O-ATPase with respect to 1.0–2.0 - 4.0–6.0 mM ATP substrate (C) in the absence (○) or with 1 mM selenite (●) and with respect to 0.25–0.5 - 1.0–2.0 mM Mg2+ cofactor (F) in the absence (□) or with 1 mM selenite (■). *K*m and *V*max values were obtained as detailed in the kinetic analyses section of Materials and Methods. Each point represents the mean ± SD from three experiments on distinct mitochondrial preparations.

hydrolyzed in the presence of oligomycin [19]. In all experiments, the F-ATPase activity, either activated by Ca^{2+} as cofactor or by Mg^{2+}, was expressed as μmol Pi•mg protein^{-1} min^{-1}.

2.4. Quantitative evaluation of free thiols

Free thiols in mitochondrial suspensions in the absence and in the presence or absence of selenite with and without ME were colourimetrically quantified by Ellman's reagent [25]. The selected compounds were added to the mitochondrial suspensions immediately before the colourimetric analysis. The widely used Ellman's method is based on the capability of 5,5′-Dithiobis(2-nitrobenzoic acid) (DTNB) to react with free thiol groups by disulphide bonds with thionitrobenzoic acid (TNB). As the ratio of protein thiols to TNB formed is 1:1, TNB formation is currently taken as a measure of the number of free thiol groups in mitochondrial suspensions. After the addition of 15 % w/v trichloroacetic acid solution (250 μL/0.15 mg protein) to precipitate proteins, the mitochondrial suspensions were centrifuged at 12,000 *g* for 5 min at 4 °C. After the removal of the supernatant, the mitochondrial pellet was carefully resuspended with a Potter Eppendorf pestle. Then, 400 μL of reagent solution containing 0.5 M phosphate buffer (KH_2PO_4/K_2HPO_4, pH 7.4), 0.2 mM DTNB, were added to the suspensions and incubated for 20 min at 4 °C. The absorbance at 412 nm (maximum TNB absorption wavelength) of the supernatant from a second centrifugation at 12,000 *g* for 5 min at 4 °C was read on a Perkin–Elmer lambda 45 spectrophotometer. Mitochondrial thiol groups were quantitatively evaluated by interpolating the absorbance values in a calibration curve built by employing known cysteine concentrations as –SH standard.

2.5. Kinetic analyses

In all plots the specific enzyme activity, evaluated as μmoles P_i•mg protein^{-1}•min^{-1}, was taken as the expression of the initial reaction rate *v*. To evaluate the enzyme activation kinetics by the ATP substrate, Hill

Table 1
Effect of selenite on the kinetic parameters of the F_1F_O-ATPase.

Kinetic parameters	ATP (substrate)		Mg^{2+} (cofactor)	
	No selenite	1 mM Selenite	No selenite	1 mM Selenite
n_{Hi} (a.u.)	2.12 ± 0.14a	1.94 ± 0.27a	1.13 ± 0.04a	1.26 ± 0.07a
$[S]_{0.5}$ (mM)	0.25 ± 0.03a	0.33 ± 0.07a	0.61 ± 0.01a	0.62 ± 0.02a
K_m (mM)	1.88 ± 0.04a	2.01 ± 0.07b	0.27 ± 0.01a	0.24 ± 0.01b
V_{max} (μmol Pi/mg protein/min)	1.39 ± 0.06a	1.63 ± 0.08b	1.79 ± 0.01a	2.19 ± 0.01b
K_a (mM)		10.78 ± 0.75*		3.64 ± 0.58*
K'_a (mM)		06.61 ± 0.47§		5.54 ± 0.74§

The values of kinetic parameters were calculated as detailed in Section 2.5. Data are the mean ± SD of n = 3 sets of experiments carried out on different mitochondrial preparations. Different letters (a, b) indicate significantly different values between the treatments with or without selenite on ATP substrate or Mg^{2+} cofactor effect. Different symbols (*, §) indicate significantly different values between the same treatment with selenite on activation constants (K_a *vs* K'_a) obtained with respect to the ATP substrate or Mg^{2+} cofactor. $P \leq 0.05$.

plots were built [26]. To this aim, Mg^{2+}-activated F-ATPase assays were carried out at various stated ATP millimolar concentrations in the reaction medium, by keeping constant all other assay conditions in the presence or in the absence of selenite. The linear transformation of the Hill equation was used:

$$log \frac{v_0}{V_{max} - v_0} = -n_{Hi}\ log[S] + log\ K' \quad \text{Eq. 1}$$

where V_{max} and v_0 represent the enzyme reaction rates, respectively in the presence of substrate concentration (ATP or Mg^{2+}) which gives the maximal rate and in the presence of a stated substrate concentration [*S*], K' or $[S]_{0.5}$ is the substrate concentration occupying half of the binding sites. By plotting log $v_0/(V_{max}\text{-}v_0)$ versus log[*S*] a straight line is obtained, whose slope is Hill coefficient ($-n_{Hi}$). In case $|n_{Hi}| \neq 1$ multiple binding sites for the substrate can be involved [26] even if the n_{Hi} value cannot stoichiometrically correspond to the binding sites.

The mechanism of the enzyme activation by selenite on the F-ATPase was explored with the aid of the graphical method of Lineweaver-Burk (double reciprocal plots). In all kinetic analyses, the enzyme-specific activity was taken as the expression of the reaction rate (v). To calculate the kinetic parameters (V_{max} and K_m) of ATP substrate or Mg^{2+} cofactor, enzyme activity data were fitted to the Lineweaver-Burk equation:

$$\frac{1}{v} = \frac{K_m}{V_{max}} \frac{1}{[S]} + \frac{1}{V_{max}} \quad \text{Eq. 2}$$

in which the reciprocal of the reaction rate $1/v$ (y-axis) was plotted as a function of the concentration of ATP or Mg^{2+} cofactor (x-axis) considered as substrate (*S*) raised to a power of n_{Hi}. This corrective procedure allows the building of linear double reciprocal plots, and consequently, the calculation of V_{max} and K_m values from the intercept with y- and x-axis, respectively, even when nHi is ≠1. Moreover, the enzyme activity stimulated by selenite fits a straight line in which the Lineweaver-Burk equation considers the factor α, $\alpha = 1 + [A]/K_a$, or α', $\alpha' = 1 + [A]/K'_a$.

$$\frac{1}{v} = \frac{\alpha K_m}{V_{max}} \frac{1}{[S]} + \frac{\alpha'}{V_{max}} \quad \text{Eq. 3}$$

The equilibrium constant for activation binding, K_a or K'_a, can be obtained from the double reciprocal plots by considering the value of α or α', respectively. K_a is the constant related to the binary complex of the free enzyme (*E*) plus activator (*A*), *i.e.*, *EA* or in other words *E* plus selenite, obtained by rearranging the value of α, $K_a = [A]/(\alpha - 1)$, whereas K'_a, calculated as $K'_a = [A]/(\alpha' - 1)$, is the constant describing the ternary complex *EA* plus *S*, *i.e.*, *ESA* or in other words *ES* plus selenite, as reported in the enzyme reactions scheme:

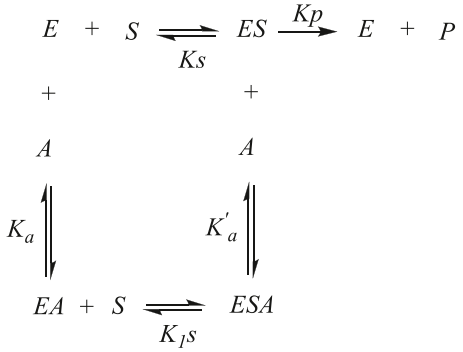

Analyzing Lineweaver-Burk plots, the α is assumed as follows: gradient of Eq. (3), $(\frac{\alpha K_m}{V_{max}})$, multiplied by the ratio of V_{max} and K_m values from Eq. (2) in the absence of selenite; the α' is assumed as follows: y-axis intercept of Eq. (3), $(\frac{\alpha'}{V_{max}})$, multiplicate by the V_{max} values of Eq. (2) in the absence of selenite.

In the plot, distinct straight lines, each of which corresponded to a fixed concentration of selenite, were obtained by linear regression. The R^2 value was never lower than 0.98, thus confirming the linearity of these plots.

2.6. Evaluation of oxidative phosphorylation

Immediately after the fresh preparation of the swine heart mitochondrial fraction, the mitochondrial respiratory activity was polarographically evaluated by a Clark-type electrode using a thermostated Oxytherm System (Hansatech Instruments, King's Lynn, UK) in terms of oxygen consumption at 37 °C in a 1 mL polarographic chamber. The reaction mixture, maintained at a fixed temperature and continuously stirred, contained a 0.25 mg/mL mitochondrial suspension, 40 mM KCl, 0.2 mg/mL fatty-acid-free BSA, 75 mM sucrose, 0.5 mM EDTA, 30 mM Tris–HCl, pH 7.4, and 5 mM KH_2PO_4, plus 3 mM $MgCl_2$. The reaction was carried out at a fixed temperature and under constant stirring. The assessment of the rate of oxygen consumption was made in the presence of specific substrates. In regard to complex I, the substrates were glutamate/malate in a ratio of 1:1; for complex II, the substrate was succinate. Furthermore, complex I was inhibited by 1 μg/mL of rotenone, while the inhibition of complex III was achieved by 1 μM of antimycin A. The oxidation of glutamate/malate made it possible to determine the activity of NADH; for ubiquinone oxidoreductase, on the other hand, the oxidation of succinate represented the multicomponent succinoxidase pathway, *i.e.*, the electron flux in the respiratory chain through complex II. By adding 1 μM of antimycin A to the respective tests with glutamate/malate and succinate, it was possible to evaluate the nonspecific oxygen consumption. To evaluate the coupling between respiratory activity and phosphorylation, 150 nmol ADP at state 2 of respiring mitochondria was added [27,28]. The respiratory control ratio (RCR) of OXPHOS was assessed as the ratio between state 3 (when ATP is synthesized) and state 4 (when ATP is not synthesized). To evaluate the effects of the selenite, the mitochondrial suspensions were added at the same time to selenite in the polarographic chamber before starting the reaction at 37 °C. Respiratory activities were expressed as nmoles O_2•mg protein^{-1} min^{-1}. The experimental protocol provided for the injection (in a very precise order) of reagents into the polarographic cell using a syringe. In particular, to mitochondrial protein suspensions, in the presence and absence of the selenite, the following were added: inhibitors of the previous respiratory chain steps (when required),

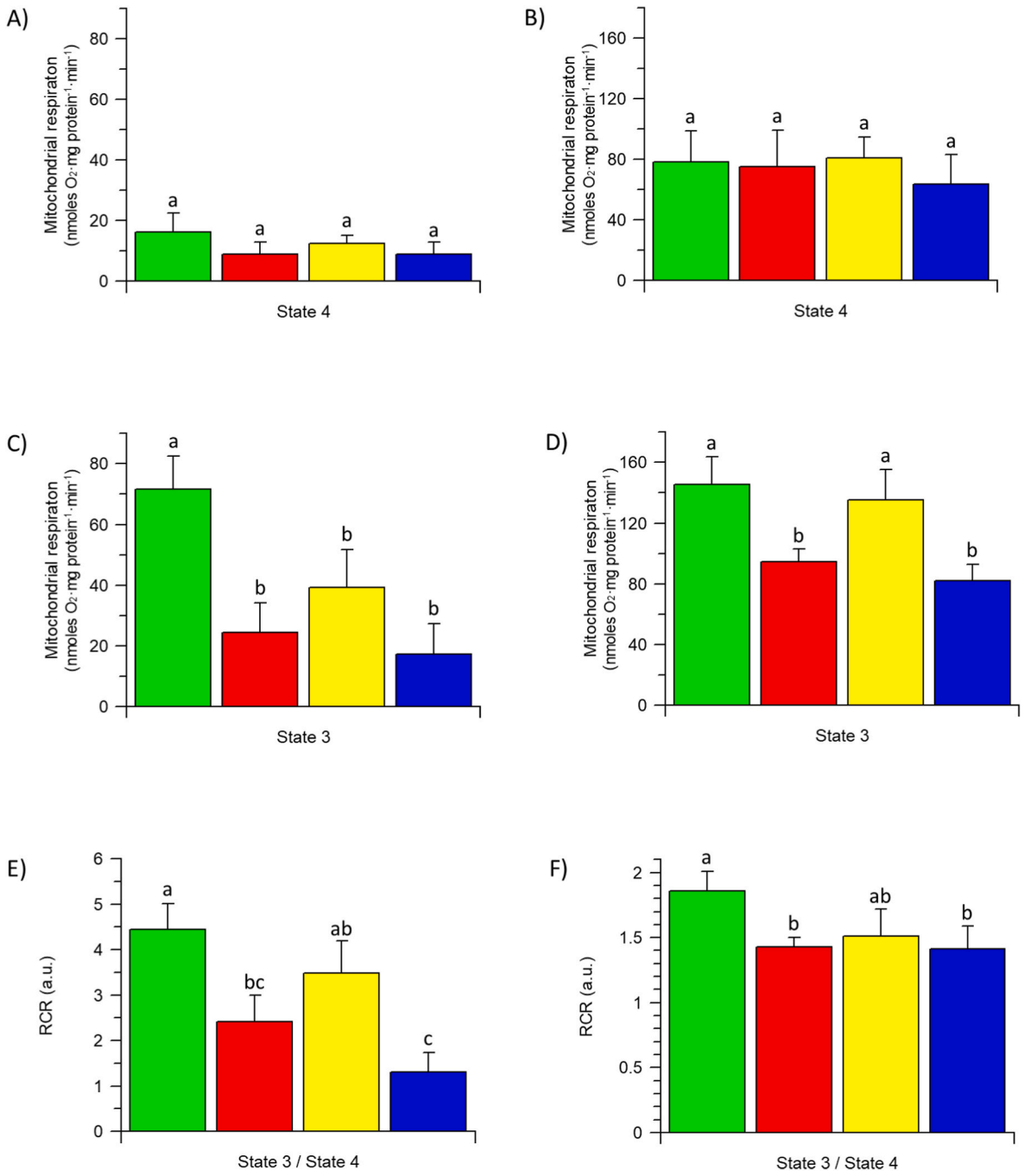

Fig. 5. Selenite effect on selected oxidative phosphorylation parameters: state 3 and 4 respiration rates and their ratio as the respiratory control ratio. Glutamate/malate- (A, C, E) and succinate- (B, D, F) stimulated mitochondrial respiration in the absence (green,) or in the presence of 1 mM selenite (red,), 50 μM DTT (yellow,), and selenite + DTT (blu,). Data expressed as columns represent the mean ± SD from three independent experiments carried out on different mitochondrial preparations. Different letters indicate significant differences ($P \leq 0.05$) among treatments within the same parameter between treatments.

substrate(s), ADP, and inhibitors (rotenone for glutamate/malate-stimulated respiration and antimycin A for succinate-stimulated respiration) [10]. The rate of oxygen consumption was assessed in the presence of the specific substrates, glutamate/malate for complex I and succinate for complex II. Polarographic assays were performed at least in triplicate on three mitochondrial preparations from different animals.

2.7. Evaluation of mPTP

Immediately after the preparation of swine heart mitochondrial fractions, fresh mitochondrial suspensions (1 mg/ml) were energized in the assay buffer (130 mM KCl, 1 mM KH_2PO_4, 20 mM HEPES, pH 7.2 with TRIS), incubated at 25 °C with 1 μg/ml rotenone and 5 mM succinate as respiratory substrate. To evaluate selenite effect, selected selenite concentrations, obtained by sampling small aliquots from standard selenite aqueous solutions were added to the mitochondrial suspensions before mPTP evaluation. mPTP opening was induced by the addition of low concentrations of Ca^{2+} (10 μM) as $CaCl_2$ aqueous solution at fixed time intervals (1 min). The Ca^{2+} retention capacity (CRC), whose lowering indicates mPTP opening, was spectrofluorophotometrically evaluated in the presence of 0.8 μM Fura-FF. The probe has

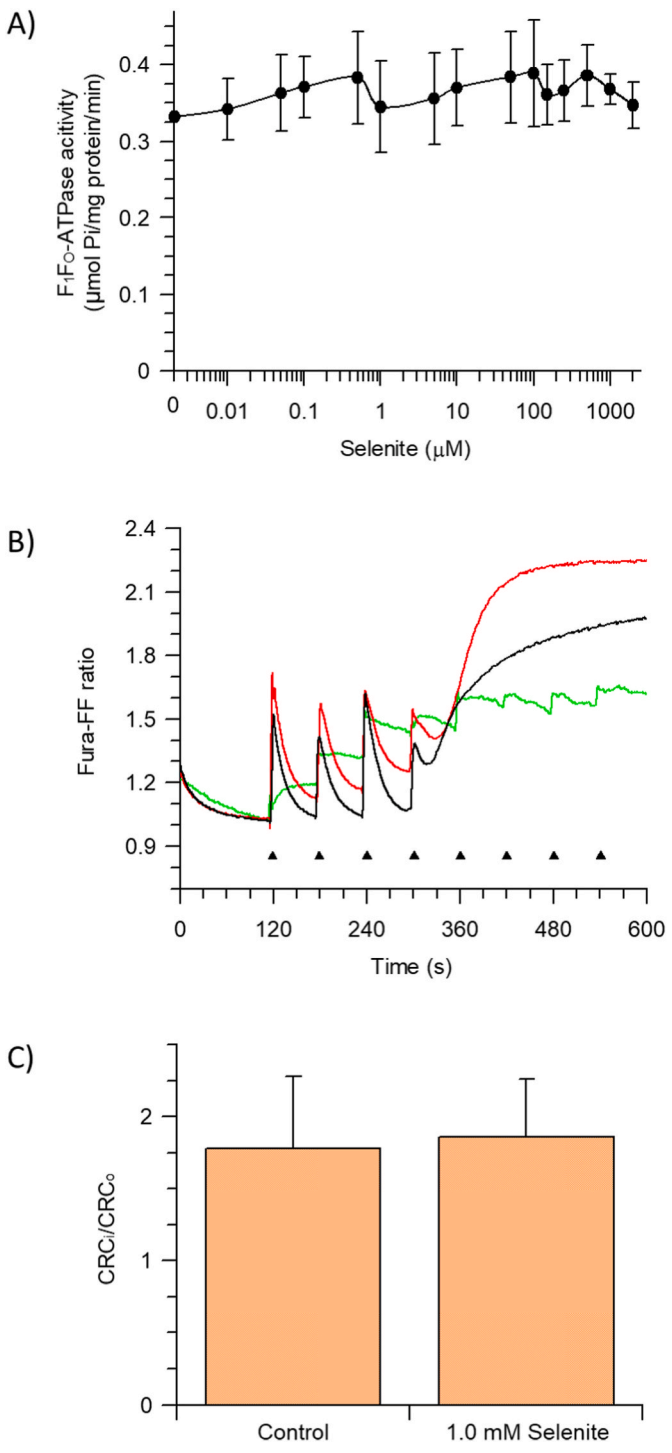

Fig. 6. Effect of selenite on the F_1F_O-ATPase activity and the mPTP opening. A) ATP hydrolysis of F_1F_O-ATPase activated by Ca^{2+} in the presence of increasing selenite concentrations. B) The calcium retention capacity (CRC) was monitored in response to subsequent 10 µM $CaCl_2$ pulses (shown by the triangles), as detailed in Section 2.7., in the absence (control, — black line), in the presence of the inhibitor 2 mM MgADP (— green line), and 1 mM selenite (— red line). C) Quantitation of the mPTP opening is expressed as the ratio of the number of calcium pulses required to induce the mPTP in MgADP-inhibited (CRC_i) and uninhibited (CRC_o) mitochondria in the absence (control) and in the presence of selenite. Data represent the mean ± SD from three independent experiments carried out on distinct mitochondrial preparations.

different spectral properties in the absence and in the presence of Ca^{2+}, namely, it displays excitation/emission spectra of 365/514 nm in the absence of Ca^{2+} (Fura-FF low Ca^{2+}) and shifts to 339/507 nm in the presence of high Ca^{2+} concentrations (Fura-FF high Ca^{2+}). mPTP opening was evaluated by the increase in the fluorescence intensity ratio (Fura-FF high Ca^{2+})/(Fura-FF low Ca^{2+}), which indicates a decrease in CRC [29]. All measurements were processed by LabSolutions RF software.

2.8. Calculations and statistics

The data represent the mean ± SD (shown as vertical bars in the figures) of the number of experiments reported in the figure captions. In each experimental set, the analyses were carried out on different pools of animals. Statistical analyses were performed by SIGMASTAT software. The analysis of variance followed by Students–Newman–Keuls' test when *F* values indicated significance ($P \leq 0.05$) was applied. Percentage data were *arcsin*-transformed before statistical analyses to ensure normality.

3. Results

3.1. Selenite affects the F_1F_O-ATPase activity by reversible modulation of thiol redox state

The effect of selenite, in the range of 0.1–2.0 mM, was evaluated on the F_1F_O-ATPase activated by Mg^{2+} as cofactor (Fig. 1). Increasing selenite concentrations promote a significant increase of ATP hydrolysis at the highest concentration tested (0.5–1.0 – 2.0 mM selenite). The enzyme attained a maximal 26 % activation at the 1.0 mM selenite.

To verify if the cysteine redox state by selenite was related to the activation effects on the F_1F_O-ATPase the thiols reagents: 50 µM DTT, 2.5 µM $HgCl_2$, 50 µM PAO, and 400 mM ME were tested. The Mg^{2+}-activated F_1F_O-ATPase activity was evaluated in the presence of 0.50–1.00 mM or in the absence of selenite (Fig. 2A–D) with and without DTT, $HgCl_2$, PAO, or ME to check if the modified cysteine thiols (-SH) of the protein adduct with selenite were reduction-sensitive. In the presence of selenite, the Mg^{2+}-activated F_1F_O-ATPase showed the same enzyme activity as with 50 µM DTT, 2.5 µM $HgCl_2$, or 50 µM PAO in the reaction medium (Fig. 2A,B,C). Conversely, the addition of 400 mM ME significantly lessened at the value of control the enzyme activity stimulated in the presence of 0.50 or 1.00 mM selenite (Fig. 2D).

Taking into account selenite's capacity to form complexes with Cys-SH, its possible binding to mitochondrial proteins was studied by measuring the –SH content in swine heart mitochondria incubated in the absence or presence of selenite with and without the ME. The number of free thiol groups in mitochondria decreased dramatically in the presence of 1 mM selenite up to 45 %. The redox state of –SH groups were not modified by 400 mM of ME, and the oxidation of –SH groups by selenite adduct was reverted by the addition of ME (Fig. 3).

3.2. Activation kinetics of selenite on F_1F_O-ATPase

The F_1F_O-ATPase mechanism of ATP hydrolysis was characterized by positive cooperativity that promoted enzyme catalysis. The activation effect of selenite was studied on enzyme cooperativity to verify if the relationship between the fraction of occupied sites and the ligand concentration was changed. The Hill plots built at different concentrations of substrate ATP in the absence and in the presence of 1 mM of selenite (Fig. 4A and B) showed similar Hill coefficients, namely 2.12 ± 0.14 and 1.94 ± 0.27 respectively (Table 1), thus suggesting that, in both cases, ATP can bind to two catalytic sites. Moreover, the binding sites of the enzyme were filled with the same concentration of ATP since the $[S]_{0.5}$ with and without selenite had the same value (Table 1). However, the F_1F_O-ATPase in the presence of selenite sustained a higher ATP hydrolysis. The molecular mechanism of enzyme activation, plotted as a

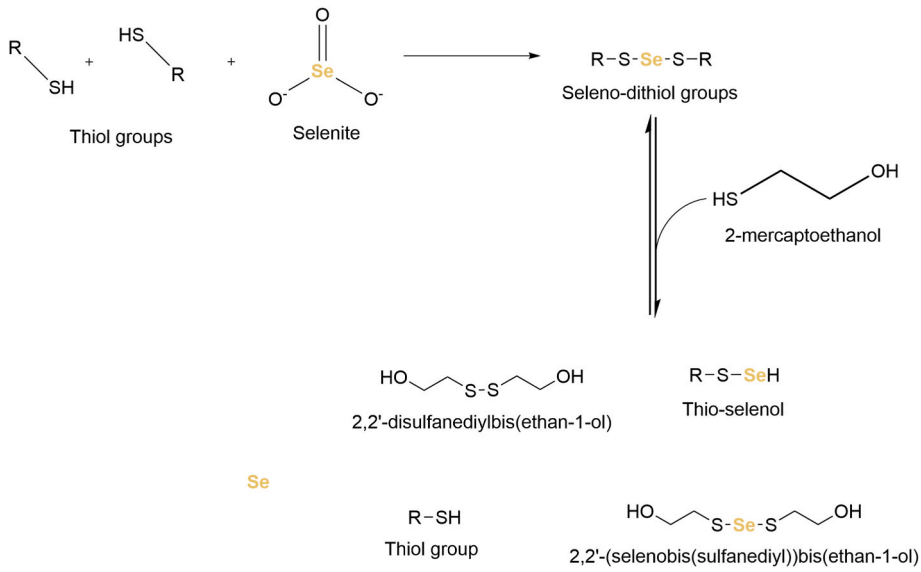

Fig. 7. Modified cysteine thiols with selenite on the protein adduct. The possible redox reactions of selenite con thiol groups of F_1F_O-ATPase and the reversible effect of ME (2-mercaptoethanol) on the seleno-dithiol groups. The possible products are depicted.

function of the concentration of ATP substrate, was an uncompetitive mixed type (Fig. 4C). Accordingly, in the presence of selenite the K_m and the V_{max} of the enzyme showed higher values than in the absence (Table 1), which indicated that when activated by selenite, the enzyme hydrolytic activity was more efficient but more substrate was required to reach one-half V_{max} increased by the factor α'. The activation mechanism of selenite was corroborated by K_a and K'_a values that describe the dissociation of binary (*EA*) and ternary (*ESA*) complexes, respectively. The K_a value higher than K'_a value indicated that selenite bound more easily to F_1F_O-ATPase complexed with ATP according to the uncompetitive mixed-type inhibition mechanism forming *ESA* complex. (Table 1). The same study has been performed in relation to the Mg^{2+} cofactor regarding the cooperativity of the enzyme (Fig. 4D and E) and the activation mechanism of selenite (Fig. 4F). The n_{Hi} values with and without selenite highlighted the absence of cooperativity to Mg^{2+} and likewise the $[S]_{0.5}$ values did not change; selenite did not affect the cofactor concentration occupying half of the binding sites (Table 1). Selenite activation of F_1F_O-ATPase was mixed competitive with respect to Mg^{2+} cofactor. On considering the activation constants of the enzyme–activator complex (K_a) and the enzyme–substrate–activator complex (K'_a), since F_1F_O-ATPase showed K_a value slightly lower than K'_a value (Table 1), the formation of the binary complex (enzyme–selenite) was preferred.

3.3. Selenite effect on oxidative phosphorylation

To assess the selenite effect on the bifunctional mechanism of F_1F_O-ATPase, the ATP synthesis coupled to the mitochondrial respiration in the OXPHOS system was studied in the presence of glutamate/malate or succinate as substrates for the first, in the Complex I (CI), or second phosphorylation sites, in the Complex II (CII), respectively, to understand the relationship between substrate oxidation by mitochondrial respiratory complexes and the selenite effect on F_1F_O-ATPase (Fig. 5). Respiration was evaluated in State 3 respiring in presence of ADP and Pi, and State 4 obtained after State 3 when added ADP is phosphorylated maximally to ATP. Moreover, the coupling between substrate oxidation and ADP phosphorylation was calculated as the RCR index obtained as State3/State4 ratio.

Mitochondrial respiration in State 4 was unaffected by selenite and/or DTT assumed that the compound and the changing redox state of –SH thiol groups of the respiratory complex were unaffected indifferently of substrates to CI or CII (Fig. 5A and B). ME, which had a reversible effect on the stimulation of ATPase activity in the presence of selenite, inhibited mitochondrial respiration (data not shown). Conversely, the selenite influenced the respiration in State 3 irrespective of the substrate to the first or second phosphorylation site. Mitochondria in State 3 energized with glutamate/malate were inhibited by 65 % with 1 mM selenite, whereas in the presence of a substrate at the second phosphorylation site, the inhibition was 35 %. Noteworthy, DTT had neither antagonistic nor synergistic effects with selenite (Fig. 5C and D). In the presence of a substrate for CI or CII, the respiratory control ratios (state 3/state 4) decreased only in the presence of selenite or selenite plus DTT by 45 % and 70 % at the first phosphorylation site and 18 % and 20 % at second phosphorylation site, respectively (Fig. 5E and F).

3.4. The action of selenite on the mitochondrial activities in the presence of Ca^{2+}

Dose-response curve of selenite on the Ca^{2+}-activated F_1F_O-ATPase highlighted a refractory response of the enzyme to selenite when the natural cofactor Mg^{2+} was replaced with Ca^{2+} (Fig. 6A). The mPTP was monitored to increased concentration of Ca^{2+} at subsequent steps to the mitochondrial suspensions evaluating the CRC, which represents the capability of intact mitochondria to accumulate Ca^{2+}. CRC decreased when the mPTP opened and was revealed by an increase in fluorescence intensity. CRC increased in control mitochondria after subsequent 10 μM Ca^{2+} additions at fixed time intervals, as revealed by an increase in the (Fura-FF high Ca^{2+})/(Fura-FF low Ca^{2+}) ratio, denoted as Fura-FF ratio in Fig. 6B. MgADP inhibited the mPTP opening and a higher CRC was registered. Mitochondrial suspensions were treated with 1 mM selenite, which corresponded to the selenite values for the stimulation of ATP hydrolysis activity (Fig. 1), and the mPTP opening sensitization to Ca^{2+} was not changed in the presence of selenite. Consistently, the mPTP formation showed the same number of Ca^{2+} pulses required to induce the mPTP formation in control mitochondria (Fig. 5B). Indeed, the mPTP formation, extent expressed as the ratio between MgADP inhibited (CRC_i) and untreated (CRC_o) mitochondria, (CRC_i/CRC_o), was unaffected by 1 mM selenite (Fig. 6C). Therefore, the selenite did not modulate the mPTP in swine heart mitochondria.

4. Discussion

The F_1F_O-ATPase has a bifunctional mechanism of ATP turnover [30–33]. The ATP hydrolysis provides the chemical force to drive the reverse function of the F_1F_O-ATPase working as H^+ pump and re-energising the IMM. On the contrary, the forward work of F_1F_O-ATPase dissipates the Δp generated with substrates oxidation during mitochondrial respiration to synthesize ATP in the OXPHOS [34–36]. The selenite has an opposite effect on the dual mode of work of the enzyme. Indeed, selenite stimulated the ATP hydrolysis of the enzyme and caused a significant decrease in the ADP phosphorylation. In practice, the activity of the Mg^{2+}-activated F_1F_O-ATPase was increased by up to 1 mM selenite by 26 %. Selenite, by boosting ATPase activity, might improve the coupling between glycolytic and Δp oscillations in non-respiring mitochondria [37,38], whereas the inhibition of the ATP synthesis is much more responsive in the presence of substrates for the first site of phosphorylation than the second site of phosphorylation.

Since selenite has the feature to change the redox state of cysteine residues of F_1F_O-ATPase modulating the enzyme activities, we have considered the thiol reaction with selenite [39] (Fig. 7). Vicinal thiols groups might be reduced to persulfide groups crosslinked by selenium and producing a new protein adduct identified as seleno-dithiol (-S-Se-S-). The modified cysteine thiols with selenite might form a bridge in which the reduction potential is so high that thiol reagents are unable to cleave the -S-Se-S- bond. Otherwise, the ME with its higher reduction potential could be able to reduce the seleno-dithiol group to free thiol groups (-SH) or form thio-selenol (Fig. 7). Indeed, these two forms can be revealed by Ellman's Reagent (DTNB) that reacts with sulfhydryl groups [19], explaining the restored effect on the quantification of free –SH in presence of selenite + ME (Fig. 3). Moreover, the ME effect reverted the activation mechanism on ATP hydrolysis of F_1F_O-ATPase but was not possible to evaluate it on the mechanism of ATP synthesis as ME inhibited mitochondrial respiration and consequently impaired the ADP phosphorylation. We can speculate that critical –SH groups sensitive to selenite modulate in the opposite way the bifunctional mechanism of F_1F_O-ATPase [40]. Reversible cysteine oxidations have versatile control of the structure and function of the F_1F_O-ATPase. Dithiol potentially responsible for -S-Se-S- adduct might be localized on the α and γ subunits [40]. Indeed, disulfide bonds can be formed between cysteines of two α subunits ($_\alpha$Cys-251) or cysteines of α and γ subunits ($_\alpha$Cys-251 and $_\gamma$Cys-78) before that the individual subunits assemble to yield the holoenzyme. Moreover, the ability to combine dithiols is determined by the conformation of the enzyme and the molecular structure of the cross-linked compound (X), which forms disulphide bridges (-S-X-S-) of varying lengths [41]. $_\alpha$Cys-201 and $_\alpha$Cys-251 is a dithiol with 14.3 Å intrasubuinit distance and $_{OSCP}$Cys-118 and $_b$Cys-197 a dithiol with 18.5 Å intersubunit distance (Fig. S1) that could potentially allow the formation of a disulfide bridge with Se.

Kinetic experiments were conducted to shed insight on the binding change process for the F_1-ATPase [42], whose ATP hydrolysis is known to be supported by the positive cooperativity of three catalytic sites. During catalysis, the ATP substrate can simultaneously fill one to three sites, denoting it as uni-site, bi-site, or tri-site catalysis, respectively [43,44]. The rate of ATP hydrolysis was ATP concentration-dependent, and selenite activated the enzyme. However, the steady-state catalysis analysis showed that the main kinetic enhancement occurs through bi-site activation maintaining positive cooperativity irrespective of the presence of selenite.

The analysis of the activation mechanism highlighted an uncompetitive mixed kinetic activation with respect to the ATP substrate. Therefore, selenite might improve the ATP binding to the enzyme by activating the ATPase activity. In general mixed kinetic activation is characterised by binary and ternary complex association described with K_a and K'_a values, respectively. The constants are representative of the affinity of the activator to bind to the free enzyme or enzyme with substrate. Since K'_a value was lower than the K_a value, selenite more efficiently complexed to form the ternary complex (*ESA*) than the binary complex (*EA*). In other words, *ESA* complex was more powerful than *EA*. Moreover, the F_1F_O-ATPase underwent a competitive mixed-type activation mechanism on the cofactor. This activation type was corroborated by a lower K_a value than K'_a value indicating that the selenite preferentially bound to the free enzyme to form the binary complex (*EA*). These results prove that selenite has a distinct site on the enzyme that does not overlap the ATP or Mg^{2+} bind site.

The F_1F_O-ATPase associates the bifunctional mechanism of energy transmission unique in biological systems [45] with the property of switching from the enzyme of life to the enzyme of death [46]. In particular, Ca^{2+}-activated F_1F_O-ATPase sustaining ATP hydrolysis could be a potential event in determining the switch to the enzyme of death through mPTP formation and opening [5,47]. However, the opposite effect of selenite on the enzyme when the hydrolysis or the synthesis of ATP was sustained by Mg^{2+} did not show either an activating effect or an inhibitory effect on the H^+-translocating Ca^{2+}-dependent F_1F_O-ATP (hydrol)ase [9]. Since compounds that affect the Ca^{2+}-activated F_1F_O-ATPase can modulate the mPTP opening [10,23,29,41,48–51] we have confirmed that the mPTP opening was similarly refractory to the presence of selenite. Probably, the selenite does not change the molecular mechanism of conformational transmission, known as "bent-pull" model [8,52], from catalytic sites of Ca^{2+} on the F_1 domain to membrane subunits of F_O domain [9,46].

To sum up, we have defined how the bifunctional mechanism of the F_1F_O-ATPase can be differently regulated through the use of selenite. 1 mM selenite stimulates ATP hydrolysis and inhibits ATP synthesis by F_1F_O-ATPase causing a depletion of ATP content in mitochondria. High dosages of sodium selenite (>1 mM) are effective in eliciting contractures in the heart and smooth muscles [53]. Indeed, healthy cardiac metabolism relies on an efficient rate of ATP fuels to support heart muscle function. Selenite effect on mitochondria is therefore toxic under normal metabolic conditions leading to a mitochondrial depletion of ATP. However, this negative action on bioenergetics does not trigger the mPTP phenomenon. Under pathophysiological conditions, the enzyme is driven to hydrolyze ATP and this activity is regulated by the IF1 subunit, which can also regulate the ATP synthesis [54]. Future studies might be addressed to evaluate the interplay of selenite on the F_1F_O-ATPase regulatory mechanism with IF1. Indeed, pro-oncogenic or anti-metastatic phenotypes have mitohormetic programs in which the interplay in the IF1/F_1F_O-ATPase axis has a relevant role [55].

Author contributions

F.O. and S.N. conceptualization; S.N. validation; C.A. investigation; F.T. methodology; F.T., F.O., E.P. and S.N. visualization; M.F. resources; S.N. supervision; F.O. and S.N. writing - original draft; all authors writing - review & editing; S.N. funding acquisition.

Declaration of competing interest

The authors declare that they have no known competing financial interests or personal relationships that could have appeared to influence the work reported in this paper.

Acknowledgements

The work was supported by Alma Idea 2022 grant (from the University of Bologna, Italy) to Salvatore Nesci.

Appendix A. Supplementary data

Supplementary data to this article can be found online at https://doi.org/10.1016/j.freeradbiomed.2023.11.041.

References

[1] S. Nesci, A. Pagliarani, C. Algieri, F. Trombetti, Mitochondrial F-type ATP synthase: multiple enzyme functions revealed by the membrane-embedded FO structure, Crit. Rev. Biochem. Mol. Biol. 55 (2020) 309–321, https://doi.org/10.1080/10409238.2020.1784084.

[2] J.L. Martin, R. Ishmukhametov, D. Spetzler, T. Hornung, W.D. Frasch, Elastic coupling power stroke mechanism of the F1-ATPase molecular motor, Proc. Natl. Acad. Sci. USA 115 (2018) 5750–5755, https://doi.org/10.1073/pnas.1803147115.

[3] Y. Niu, S. Moghimyfiroozabad, S. Safaie, Y. Yang, E.A. Jonas, K.N. Alavian, Phylogenetic profiling of mitochondrial proteins and integration analysis of bacterial transcription units suggest evolution of F1Fo ATP synthase from multiple modules, J. Mol. Evol. 85 (2017) 219–233, https://doi.org/10.1007/s00239-017-9819-3.

[4] W. Junge, N. Nelson, ATP synthase, Annu. Rev. Biochem. 84 (2015) 631–657, https://doi.org/10.1146/annurev-biochem-060614-034124.

[5] S. Nesci, A. Pagliarani, Incoming news on the F-type ATPase structure and functions in mammalian mitochondria, BBA Advances 1 (2021), 100001, https://doi.org/10.1016/j.bbadva.2020.100001.

[6] S. Nesci, F. Trombetti, A. Pagliarani, V. Ventrella, C. Algieri, G. Tioli, G. Lenaz, Molecular and supramolecular structure of the mitochondrial oxidative phosphorylation system: implications for pathology, Life 11 (2021) 242, https://doi.org/10.3390/life11030242.

[7] P. Mitchell, J. Moyle, Respiration-driven proton translocation in rat liver mitochondria, Biochem. J. 105 (1967) 1147–1162.

[8] G. Pinke, L. Zhou, L.A. Sazanov, Cryo-EM structure of the entire mammalian F-type ATP synthase, Nat. Struct. Mol. Biol. 27 (2020) 1077–1085, https://doi.org/10.1038/s41594-020-0503-8.

[9] S. Nesci, A. Pagliarani, Ca2+ as cofactor of the mitochondrial H+-translocating F1FO-ATP(hydrol)ase, Proteins, Structure, Function, and Bioinformatics 89 (2021) 477–482, https://doi.org/10.1002/prot.26040.

[10] C. Algieri, C. Bernardini, F. Oppedisano, D. La Mantia, F. Trombetti, E. Palma, M. Forni, V. Mollace, G. Romeo, S. Nesci, Mitochondria bioenergetic functions and cell metabolism are modulated by the bergamot polyphenolic fraction, Cells 11 (2022) 1401, https://doi.org/10.3390/cells11091401.

[11] C. Algieri, C. Bernardini, F. Oppedisano, D. La Mantia, F. Trombetti, E. Palma, M. Forni, V. Mollace, G. Romeo, I. Troisio, S. Nesci, The impairment of cell metabolism by cardiovascular toxicity of doxorubicin is reversed by bergamot polyphenolic fraction treatment in endothelial cells, Int. J. Mol. Sci. 23 (2022) 8977, https://doi.org/10.3390/ijms23168977.

[12] M. Kieliszek, Selenium¯Fascinating microelement, properties and sources in food, Molecules 24 (2019) 1298, https://doi.org/10.3390/molecules24071298.

[13] M.P. Rayman, The importance of selenium to human health, Lancet 356 (2000) 233–241, https://doi.org/10.1016/S0140-6736(00)02490-9.

[14] B. Hosnedlova, M. Kepinska, S. Skalickova, C. Fernandez, B. Ruttkay-Nedecky, T. D. Malevu, J. Sochor, M. Baron, M. Melcova, J. Zidkova, R. Kizek, A summary of new findings on the biological effects of selenium in selected animal species-A critical review, Int. J. Mol. Sci. 18 (2017) 2209, https://doi.org/10.3390/ijms18102209.

[15] J. Li, L. Zuo, T. Shen, C. Xu, Z. Zhang, Induction of apoptosis by sodium selenite in human acute promyelocytic leukemia NB4 cells: involvement of oxidative stress and mitochondria, J. Trace Elem. Med. Biol. 17 (2003) 19–26, https://doi.org/10.1016/S0946-672X(03)80041-X.

[16] N. Mendelev, S.L. Mehta, H. Idris, S. Kumari, P.A. Li, Selenite stimulates mitochondrial biogenesis signaling and enhances mitochondrial functional performance in murine hippocampal neuronal cells, PLoS One 7 (2012), e47910, https://doi.org/10.1371/journal.pone.0047910.

[17] M. Wojewoda, J. Duszyński, M. Więckowski, J. Szczepanowska, Effect of selenite on basic mitochondrial function in human osteosarcoma cells with chronic mitochondrial stress, Mitochondrion 12 (2012) 149–155, https://doi.org/10.1016/j.mito.2011.06.010.

[18] O.D. Jarman, O. Biner, J. Hirst, Regulation of ATP hydrolysis by the ε subunit, ζ subunit and Mg-ADP in the ATP synthase of Paracoccus denitrificans, Biochim. Biophys. Acta Bioenerg. 1862 (2021), 148355, https://doi.org/10.1016/j.bbabio.2020.148355.

[19] S. Nesci, V. Ventrella, F. Trombetti, M. Pirini, A. Pagliarani, The mitochondrial F1FO-ATPase desensitization to oligomycin by tributyltin is due to thiol oxidation, Biochimie 97 (2014) 128–137, https://doi.org/10.1016/j.biochi.2013.10.002.

[20] M.M. Bradford, A rapid and sensitive method for the quantitation of microgram quantities of protein utilizing the principle of protein-dye binding, Anal. Biochem. 72 (1976) 248–254, https://doi.org/10.1006/abio.1976.9999.

[21] S. Nesci, F. Trombetti, V. Ventrella, M. Pirini, A. Pagliarani, Kinetic properties of the mitochondrial F1FO-ATPase activity elicited by Ca(2+) in replacement of Mg(2+), Biochimie 140 (2017) 73–81, https://doi.org/10.1016/j.biochi.2017.06.013.

[22] C. Algieri, F. Trombetti, A. Pagliarani, V. Ventrella, C. Bernardini, M. Fabbri, M. Forni, S. Nesci, Mitochondrial Ca2+ -activated F1 FO -ATPase hydrolyzes ATP and promotes the permeability transition pore, Ann. N. Y. Acad. Sci. 1457 (2019) 142–157, https://doi.org/10.1111/nyas.14218.

[23] C. Algieri, F. Trombetti, A. Pagliarani, V. Ventrella, S. Nesci, Phenylglyoxal inhibition of the mitochondrial F1FO-ATPase activated by Mg2+ or by Ca2+ provides clues on the mitochondrial permeability transition pore, Arch. Biochem. Biophys. 681 (2020), 108258, https://doi.org/10.1016/j.abb.2020.108258.

[24] V. Ventrella, S. Nesci, F. Trombetti, P. Bandiera, M. Pirini, A.R. Borgatti, A. Pagliarani, Tributyltin inhibits the oligomycin-sensitive Mg-ATPase activity in Mytilus galloprovincialis digestive gland mitochondria, Comp. Biochem. Physiol. C Toxicol. Pharmacol. 153 (2011) 75–81, https://doi.org/10.1016/j.cbpc.2010.08.007.

[25] G.L. Ellman, Tissue sulfhydryl groups, Arch. Biochem. Biophys. 82 (1959) 70–77, https://doi.org/10.1016/0003-9861(59)90090-6.

[26] I.H. Segel, Enzyme kinetics, in: W.J. Lennarz, M.D. Lane (Eds.), Encyclopedia of Biological Chemistry, Academic Press, Waltham, 2013, pp. 216–220, https://doi.org/10.1016/B978-0-12-378630-2.00012-8.

[27] B. Chance, G.R. Williams, W.F. Holmes, J. Higgins, Respiratory enzymes in oxidative phosphorylation. V. A mechanism for oxidative phosphorylation, J. Biol. Chem. 217 (1955) 439–451.

[28] B. Chance, G.R. Williams, Respiratory enzymes in oxidative phosphorylation. III. The steady state, J. Biol. Chem. 217 (1955) 409–427.

[29] S. Nesci, C. Algieri, F. Trombetti, V. Ventrella, M. Fabbri, A. Pagliarani, Sulfide affects the mitochondrial respiration, the Ca2+-activated F1FO-ATPase activity and the permeability transition pore but does not change the Mg2+-activated F1FO-ATPase activity in swine heart mitochondria, Pharmacol. Res. 166 (2021), 105495, https://doi.org/10.1016/j.phrs.2021.105495.

[30] P. Dimroth, C. von Ballmoos, T. Meier, Catalytic and mechanical cycles in F-ATP synthases. Fourth in the cycles review series, EMBO Rep. 7 (2006) 276–282, https://doi.org/10.1038/sj.embor.7400646.

[31] S. Nesci, F. Trombetti, V. Ventrella, A. Pagliarani, The a subunit asymmetry dictates the two opposite rotation directions in the synthesis and hydrolysis of ATP by the mitochondrial ATP synthase, Med. Hypotheses 84 (2015) 53–57, https://doi.org/10.1016/j.mehy.2014.11.015.

[32] S. Nesci, F. Trombetti, V. Ventrella, A. Pagliarani, Opposite rotation directions in the synthesis and hydrolysis of ATP by the ATP synthase: hints from a subunit asymmetry, J. Membr. Biol. 248 (2015) 163–169, https://doi.org/10.1007/s00232-014-9760-y.

[33] H. Itoh, A. Takahashi, K. Adachi, H. Noji, R. Yasuda, M. Yoshida, K. Kinosita, Mechanically driven ATP synthesis by F1-ATPase, Nature 427 (2004) 465–468, https://doi.org/10.1038/nature02212.

[34] W. Junge, H. Lill, S. Engelbrecht, ATP synthase: an electrochemical transducer with rotatory mechanics, Trends Biochem. Sci. 22 (1997) 420–423, https://doi.org/10.1016/S0968-0004(97)01129-8.

[35] M. Yoshida, E. Muneyuki, T. Hisabori, ATP synthase–a marvellous rotary engine of the cell, Nat. Rev. Mol. Cell Biol. 2 (2001) 669–677, https://doi.org/10.1038/35089509.

[36] P.D. Boyer, The ATP synthase–a splendid molecular machine, Annu. Rev. Biochem. 66 (1997) 717–749, https://doi.org/10.1146/annurev.biochem.66.1.717.

[37] L.F. Olsen, A.Z. Andersen, A. Lunding, J.C. Brasen, A.K. Poulsen, Regulation of glycolytic oscillations by mitochondrial and plasma membrane H+-ATPases, Biophys. J. 96 (2009) 3850–3861, https://doi.org/10.1016/j.bpj.2009.02.026.

[38] S. Nesci, F. Trombetti, M. Pirini, V. Ventrella, A. Pagliarani, Mercury and protein thiols: stimulation of mitochondrial F1FO-ATPase and inhibition of respiration, Chem. Biol. Interact. 260 (2016) 42–49, https://doi.org/10.1016/j.cbi.2016.10.018.

[39] J.L. Kice, T.W.S. Lee, S.-T. Pan, Mechanism of the reaction of thiols with selenite, J. Am. Chem. Soc. 102 (1980) 4448–4455, https://doi.org/10.1021/ja00533a025.

[40] S. Nesci, F. Trombetti, V. Ventrella, A. Pagliarani, Post-translational modifications of the mitochondrial F1FO-ATPase, Biochim. Biophys. Acta 1861 (2017) 2902–2912, https://doi.org/10.1016/j.bbagen.2017.08.007.

[41] C. Algieri, F. Trombetti, A. Pagliarani, V. Ventrella, S. Nesci, The mitochondrial F1FO-ATPase exploits the dithiol redox state to modulate the permeability transition pore, Arch. Biochem. Biophys. 712 (2021), 109027, https://doi.org/10.1016/j.abb.2021.109027.

[42] P.D. Boyer, Catalytic site occupancy during ATP synthase catalysis, FEBS Lett. 512 (2002) 29–32, https://doi.org/10.1016/S0014-5793(02)02293-7.

[43] Y.M. Milgrom, R.L. Cross, Rapid hydrolysis of ATP by mitochondrial F1-ATPase correlates with the filling of the second of three catalytic sites, Proc. Natl. Acad. Sci. U.S.A. 102 (2005) 13831–13836, https://doi.org/10.1073/pnas.0507139102.

[44] C. Algieri, S. Nesci, F. Trombetti, M. Fabbri, V. Ventrella, A. Pagliarani, Mitochondrial F1FO-ATPase and permeability transition pore response to sulfide in the midgut gland of Mytilus galloprovincialis, Biochimie 180 (2021) 222–228, https://doi.org/10.1016/j.biochi.2020.11.012.

[45] D. Okuno, R. Iino, H. Noji, Rotation and structure of FoF1-ATP synthase, J. Biochem. 149 (2011) 655–664, https://doi.org/10.1093/jb/mvr049.

[46] S. Nesci, What happens when the mitochondrial H+-translocating F1FO-ATP (hydrol)ase becomes a molecular target of calcium? The pore opens, Biochimie 198 (2022) 92–95, https://doi.org/10.1016/j.biochi.2022.03.012.

[47] S. Nesci, Mitochondrial permeability transition, F_1F_O-ATPase and calcium: an enigmatic triangle, EMBO Rep. 18 (2017) 1265–1267, https://doi.org/10.15252/embr.201744570.

[48] V. Algieri, C. Algieri, P. Costanzo, G. Fiorani, A. Jiritano, F. Olivito, M.A. Tallarida, F. Trombetti, L. Maiuolo, A. De Nino, S. Nesci, Novel regioselective synthesis of 1,3,4,5-tetrasubstituted pyrazoles and biochemical valuation on F1FO-ATPase and mitochondrial permeability transition pore formation, Pharmaceutics 15 (2023) 498, https://doi.org/10.3390/pharmaceutics15020498.

[49] V. Algieri, C. Algieri, L. Maiuolo, A. De Nino, A. Pagliarani, M.A. Tallarida, F. Trombetti, S. Nesci, 1,5-Disubstituted-1,2,3-triazoles as inhibitors of the mitochondrial Ca2+ -activated F1 FO -ATP(hydrol)ase and the permeability transition pore, Ann. N. Y. Acad. Sci. 1485 (2021) 43–55, https://doi.org/10.1111/nyas.14474.

[50] C. Algieri, C. Bernardini, S. Marchi, M. Forte, M.A. Tallarida, F. Bianchi, D. La Mantia, V. Algieri, R. Stanzione, M. Cotugno, P. Costanzo, F. Trombetti, L. Maiuolo, M. Forni, A. De Nino, F. Di Nonno, S. Sciarretta, M. Volpe, S. Rubattu, S. Nesci, 1,5-disubstituted-1,2,3-triazoles counteract mitochondrial dysfunction acting on F1FO-

ATPase in models of cardiovascular diseases, Pharmacol. Res. 187 (2023), 106561, https://doi.org/10.1016/j.phrs.2022.106561.
[51] C. Algieri, F. Trombetti, A. Pagliarani, M. Fabbri, S. Nesci, The inhibition of gadolinium ion (Gd3+) on the mitochondrial F1FO-ATPase is linked to the modulation of the mitochondrial permeability transition pore, Int. J. Biol. Macromol. 184 (2021) 250–258, https://doi.org/10.1016/j.ijbiomac.2021.06.065.
[52] N. Mnatsakanyan, E.A. Jonas, ATP synthase c-subunit ring as the channel of mitochondrial permeability transition: regulator of metabolism in development and degeneration, J. Mol. Cell. Cardiol. 144 (2020) 109–118, https://doi.org/10.1016/j.yjmcc.2020.05.013.
[53] B. Turan, E. Koç, O. Hotomaroglu, E. Kiziltan, S. Yildirim, E. Demirel, Tissue and concentration-dependent effects of sodium selenite on muscle contraction, Biol. Trace Elem. Res. 62 (1998) 265–280, https://doi.org/10.1007/BF02783976.
[54] J. García-Bermúdez, J.M. Cuezva, The ATPase Inhibitory Factor 1 (IF1): a master regulator of energy metabolism and of cell survival, Biochim. Biophys. Acta 1857 (2016) 1167–1182, https://doi.org/10.1016/j.bbabio.2016.02.004.
[55] S. Domínguez-Zorita, J.M. Cuezva, The mitochondrial ATP synthase/IF1 Axis in cancer progression: targets for therapeutic intervention, Cancers 15 (2023) 3775, https://doi.org/10.3390/cancers15153775.